PRODUCTION OF OPEN AND HIDDEN CHARM IN FIXED-TARGET EXPERIMENTS AT THE LHC*

Antoni Szczurek [a,b], Anna Cisek [b], Rafał Maciuła [a]

[a]Institute of Nuclear Physics Polish Academy of Sciences
Radzikowskiego 152, 31-342 Kraków, Poland
[b]Faculty of Exact and Technical Sciences, University of Rzeszów
35-310 Rzeszów, Poland

Received 20 March 2025, accepted 31 March 2025,
published online 26 June 2025

We discuss the production of D mesons and J/ψ quarkonia in proton–nucleus collisions in the fixed-target LHCb experiment. We consider gluon–gluon fusion within $k_{\rm t}$-factorization, processes initiated by intrinsic charm in the nucleon and perturbative recombination mechanism. All the mechanisms seem to be necessary to describe the LHCb experimental data. We get an upper limit for the probability of the large-x $c\bar{c}$ Fock component in the nucleon, which is slightly less than 1%. The recombination mechanism allows for the description of D^0 and $\bar{D}^0$ asymmetry observed by the LHCb Collaboration. We also discuss the production of J/ψ quarkonia, including colour singlet mechanisms. We include $g^*g^* \to J/\psi g$ and $g^*g^* \to \chi_c(1^+, 2^+)(\to J/\psi\gamma)$ within $k_{\rm t}$-factorization approach. Different unintegrated gluon distributions from the literature are used. A reasonable agreement is achieved with some gluon distributions from the literature.

DOI:10.5506/APhysPolBSupp.18.5-A30

1. Introduction

There is a rich program at the LHCb to study the production of open charm (D mesons) and hidden charm (charmonia). At the LHC collider mode, the gluon–gluon fusion is the dominant process. In the collinear approach, rather higher-order processes have to be included. In the $k_{\rm t}$-factorization approach, the already lowest-order approach gives a reasonable description of the data [1]. There is an interesting issue of the intrinsic charm in the nucleon which is very difficult to be predicted from first principles. While the shape of x-distribution was predicted, *e.g.* by Brodsky and collaborators [2], the absolute normalization related to probability to find

* Presented by A. Szczurek at the 31st Cracow Epiphany Conference on the *Recent LHC Results*, Kraków, Poland, 13–17 January, 2025.

the $c\bar{c}$ component must be obtained by analysing experimental data. One possibility is to study large-energy muon neutrinos measured, *e.g.* by the Ice Cube Collaboration in Antarctica. Recently, an interesting option to measure τ neutrinos in the LHC collider mode was proposed [3]. Here, we review our recent papers on fixed-target experiments, which is another option to address the issue of the intrinsic charm. The fixed-target experiments with the energy of $\sqrt{s} < 100$ GeV have observed asymmetry in the production of D^0 and $\bar{D}^0$. This observation is difficult to explain in terms of the intrinsic charm in the nucleon, as discussed in our recent papers.

The production of quarkonia, especially J/ψ, is not fully understood so far. In general, there are colour singlet and colour octet mechanisms. While the colour singlet mechanism in the $k_{\rm t}$-factorization approach is under better control [4], the colour octet contribution is usually fitted to the experimental data. Usually, new data require a new fit of long-distance matrix elements. Very recently, also J/ψ was measured in fixed-target $p + A$ collisions. We wish to discuss the situation at the lower energies (fixed-target experiments). We will discuss whether the approach discussed in [5] can allow for the description of the fixed-target LHCb data. Our study provides a test of unintegrated gluon distributions at larger longitudinal momentum fraction.

2. Mechanisms considered

The presented results were obtained taking into account several mechanisms described shortly below.

2.1. $g + g \to c + \bar{c}$ mechanism

At higher energies, relevant for the LHC, the dominant mechanism of charm/anti-charm production is the gluon–gluon fusion (see Fig. 1). In the collinear approach, one has to go to the NNLO approach to get reliable cross sections. The $k_{\rm t}$-factorization approach is an efficient way to include higher-order corrections. In this approach, the differential cross section can be written as

$$\frac{{\rm d}\sigma}{{\rm d}y_1\,{\rm d}y_2\,{\rm d}^2p_{1,{\rm t}}\,{\rm d}^2p_{2,{\rm t}}} = \int \frac{{\rm d}^2k_{1,{\rm t}}}{\pi}\frac{{\rm d}^2k_{2,{\rm t}}}{\pi}\frac{1}{16\pi^2(x_1x_2s)^2}\,\overline{|\mathcal{M}_{g^*g^*\to Q\bar{Q}}|^2}$$
$$\times\delta^2\left(\vec{k}_{1,{\rm t}} + \vec{k}_{2,{\rm t}} - \vec{p}_{1,{\rm t}} - \vec{p}_{2,{\rm t}}\right)\,\mathcal{F}_g\left(x_1, k_{1,{\rm t}}^2, \mu\right)\mathcal{F}_g\left(x_2, k_{2,{\rm t}}^2, \mu\right)\,. \qquad (1)$$

Above, $\overline{|\mathcal{M}_{g^*g^*\to Q\bar{Q}}|^2}$ is the off-shell matrix element squared for $g^*g^* \to c\bar{c}$ and $\mathcal{F}_g(x, k_{\rm t}^2, \mu)$ are the transverse-momentum-dependent, unintegrated PDFs (uPDFs).

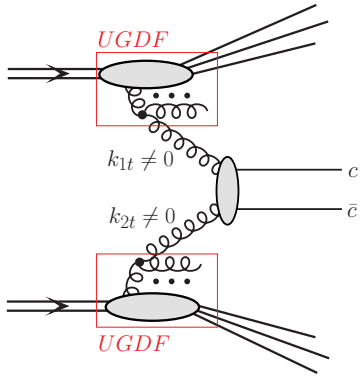

Fig. 1. Fusion of two off-shell gluons.

2.2. Charm production driven by the intrinsic charm

The differential cross section for $cg^* \to cg$ mechanism (see Fig. 2) can be written as

$$\mathrm{d}\sigma_{pp\to\mathrm{charm}}(cg^* \to cg) = \int \mathrm{d}x_1 \int \frac{\mathrm{d}x_2}{x_2} \int \mathrm{d}^2k_\mathrm{t} \times c\left(x_1,\mu^2\right)\, \mathcal{F}_g\left(x_2,k_\mathrm{t}^2,\mu^2\right)\, \mathrm{d}\hat{\sigma}_{cg^*\to cg}\,. \quad (2)$$

Above, $c(x_1,\mu^2)$ is the collinear charm quark PDF (large-x), while $\mathcal{F}_g(x_2,k_\mathrm{t}^2,\mu^2)$ is the unintegrated gluon distribution uPDF relevant at small-x.

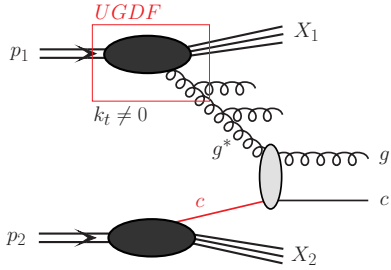

Fig. 2. A mechanism driven by the intrinsic charm.

2.3. Recombination mechanism

In our recent studies, we considered the Braaten–Jia–Mechen (BJM) perturbative model [6] of D-meson production as illustrated in Fig. 3.

In this approach, first, the $q+g \to (\bar{c}q)^n + c$ reaction is considered, where q and $\bar{c}$ are in a state with definite colour and angular momentum quantum numbers specified by n which leads to a subsequent production of a given D meson.

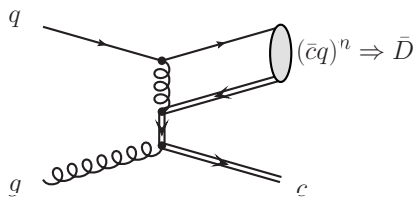

Fig. 3. A sketch of the recombination mechanism.

In addition to direct D-meson production, we have to consider also fragmentation of the associated c quark.

In the leading-order collinear approach, the differential cross section for the $qg \to \bar{D}c$ mechanism can be written as

$$\frac{\mathrm{d}\sigma}{\mathrm{d}y_1\,\mathrm{d}y_2\,\mathrm{d}^2p_\mathrm{t}} = \frac{1}{16\pi^2\hat{s}^2}\left[x_1q_1\left(x_1,\mu^2\right)x_2g_2\left(x_2,\mu^2\right)\overline{|\mathcal{M}_{qg\to\bar{D}c}(s,t,u)|^2}\right.$$
$$\left.+x_1g_1\left(x_1,\mu^2\right)x_2q_2\left(x_2,\mu^2\right)\overline{|\mathcal{M}_{gq\to\bar{D}c}(s,t,u)|^2}\right]. \quad (3)$$

Above,

$$\overline{|\mathcal{M}_{qg\to Dc}(s,t,u)|^2} = \overline{|\mathcal{M}_{qg\to(\bar{c}q)^nc}|^2}\,\rho\,. \quad (4)$$

Explicit form of the matrix element squared $\overline{|\mathcal{M}_{qg\to(\bar{c}q)^nc}|^2}$ is available in [6]. ρ above can be interpreted as a probability to form real meson D and can be extracted by confronting theoretical results with experimental data.

3. Selected results for D-meson production

In [1, 7] and [8], we presented many detailed results. Here we show only some selected results from [8].

In Figs. 4 and 5, we show rapidity and transverse-momentum distributions of $D^0 + \bar{D}^0$ mesons for two different models of intrinsic charm: BHPS (Brodsky–Hoyer–Peterson–Sakata) and MBM (meson–baryon model). The results from the two models of intrinsic charm are rather similar, so it may be rather difficult to answer the question of which model is preferred by the SMOG LHCb data. The inclusion of the intrinsic charm-initiated contributions improves the description of the fixed-target experimental data. The normalization of the intrinsic charm component ($\sim 1\%$) here is adjusted to the data.

We wish to show also asymmetry defined as

$$A = \frac{\sigma_{D^0} - \sigma_{\bar{D}^0}}{\sigma_{D^0} + \sigma_{\bar{D}^0}}\,. \quad (5)$$

We describe the experimental asymmetry with the canonical value $\rho \approx 0.1$ (see Fig. 6).

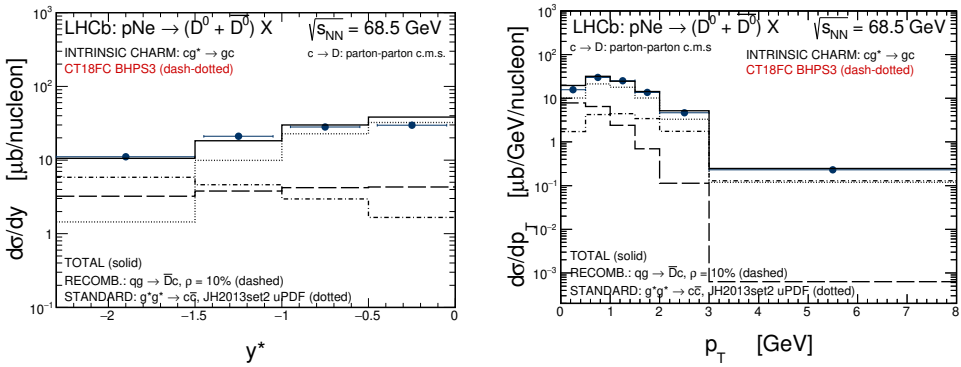

Fig. 4. Rapidity and transverse-momentum distributions of $D^0 + \bar{D}^0$ for the BHPS model of intrinsic charm.

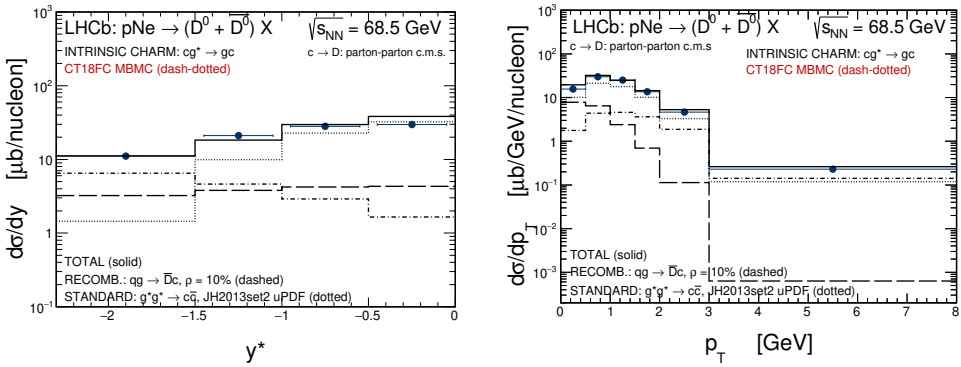

Fig. 5. Rapidity and transverse-momentum distribution of $D^0 + \bar{D}^0$ for the meson cloud model for the intrinsic charm.

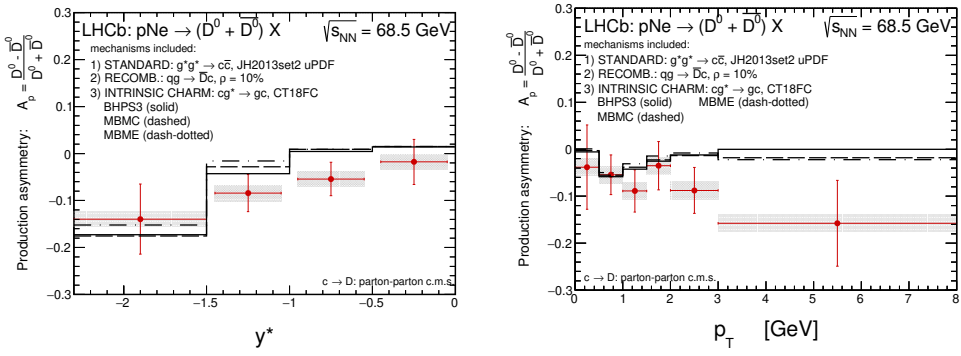

Fig. 6. Asymmetry as a function of D-meson rapidity (left) and transverse momentum (right).

In summary, we can well describe the fixed-target LHCb data with $P \approx 1\%$ and $\rho \approx 0.1$. The value of the probability found here is almost the same as found in other processes (see *e.g.* [9]).

4. $pp \to J/\psi$

The production of J/ψ in proton–proton collisions is known as a rather challenging task. Different authors use different long-distance matrix elements to get a satisfactory description of the data. Here, we shall concentrate on prompt J/ψ production, *i.e.* the decays of $B, \bar{B}$ will be neglected. The direct production is not sufficient and one has to include also decays of other quarkonia which give a sizable contribution.

Some time ago, we showed that the $k_{\rm t}$-factorization approach with non-relativistic approximation and unintegrated gluon distributions provides quite a good description of the world data [4]. This is because the $k_{\rm t}$-factorization approach includes effectively higher-order corrections. In the present studies, we wish to test how good is such an approach at lower energies. A few years ago, the LHCb Collaboration presented the first result for fixed-target experiments using the so-called SMOG device. So far, the unintegrated UGDFs have been tested in different processes rather at energies for which one is sensitive to the region of not too high longitudinal momentum fraction carried by gluon in the proton (nucleon). The region of UGDFs at larger values of x was not well tested so far. Therefore, the relatively new fixed-target data give a chance for such tests.

We calculate the dominant colour-singlet $gg \to J/\psi g$ contribution (see Fig. 7) taking into account the transverse momenta of initial gluons.

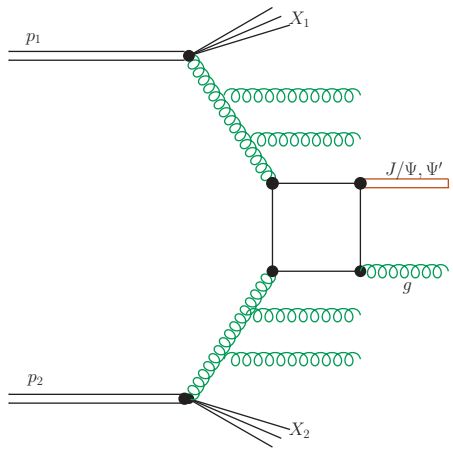

Fig. 7. The diagram for direct J/ψ (ψ') meson production in the $k_{\rm t}$-factorization approach.

In the $k_{\rm t}$-factorization approach, the differential cross section can be written as

$$\frac{{\rm d}\sigma(pp \to J/\psi g X)}{{\rm d}y_{J/\psi}\,{\rm d}y_g\,{\rm d}^2p_{J/\psi,{\rm t}}\,{\rm d}^2p_{g,{\rm t}}} = \frac{1}{16\pi^2\hat{s}^2}\int \frac{{\rm d}^2q_{1{\rm t}}}{\pi}\frac{{\rm d}^2q_{2{\rm t}}}{\pi}\overline{|\mathcal{M}^{\rm off-shell}_{g^*g^*\to J/\psi g}|^2}$$
$$\times\delta^2\left(\vec{q}_{1{\rm t}}+\vec{q}_{2{\rm t}}-\vec{p}_{H,{\rm t}}-\vec{p}_{g,{\rm t}}\right)\mathcal{F}_g\left(x_1,q_{1{\rm t}}^2,\mu^2\right)\mathcal{F}_g\left(x_2,q_{2{\rm t}}^2,\mu^2\right)\,, \tag{6}$$

where $\mathcal{F}_g$ are the unintegrated gluon distributions functions.

The corresponding matrix element squared for the $gg \to J/\psi g$ is

$$|\mathcal{M}_{gg\to J/\psi g}|^2 \propto \alpha_{\rm s}^3|R(0)|^2\,. \tag{7}$$

In the $k_{\rm t}$-factorization approach, the leading-order cross section for the χ_c-meson production (see Fig. 8) can be written somewhat formally as

$$\sigma_{pp\to\chi_c} = \int \frac{{\rm d}x_1}{x_1}\frac{{\rm d}x_2}{x_2}\frac{{\rm d}^2q_{1{\rm t}}}{\pi}\frac{{\rm d}^2q_{2{\rm t}}}{\pi}\delta\left((q_1+q_2)^2-M_{\chi_c}^2\right)\sigma_{gg\to H}\left(x_1,x_2,q_1,q_2\right)$$
$$\times\mathcal{F}_g\left(x_1,q_{1{\rm t}}^2,\mu_{\rm F}^2\right)\mathcal{F}_g\left(x_2,q_{2{\rm t}}^2,\mu_{\rm F}^2\right)\,, \tag{8}$$

where $\mathcal{F}_g$ are the unintegrated (or transverse-momentum-dependent) gluon distributions and $\sigma_{gg\to\chi_c}$ is the $gg \to \chi_c$ (off-shell) cross section.

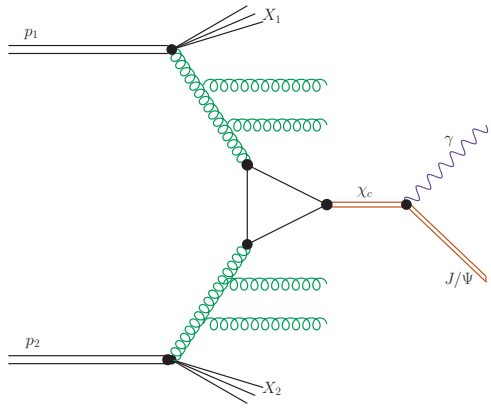

Fig. 8. The diagram for direct J/ψ (ψ') meson production in the $k_{\rm t}$-factorization approach.

In our recent analysis [5], we made calculations with the following unintegrated gluon distribution functions used previously in the literature:

(a) Kimber–Martin–Ryskin (KMR),

(b) Jung–Hautmann (JH2013),

(c) Gaussian with $\sigma = 0.5$ GeV and CTEQ-Tea Parton Distribution Functions,

(d) Kharzeev–Levin (KL),

(e) Kutak–Stasto (KS),

(f) Moriggi–Peccini–Machado (MPM).

In Fig. 9 and Fig. 10, we show our results for rapidity and transverse momentum distributions for different unintegrated gluon distributions.

For some UGDFs, the cross section is too small, for others, it is much too large, but for some of them the results are close to the experimental data.

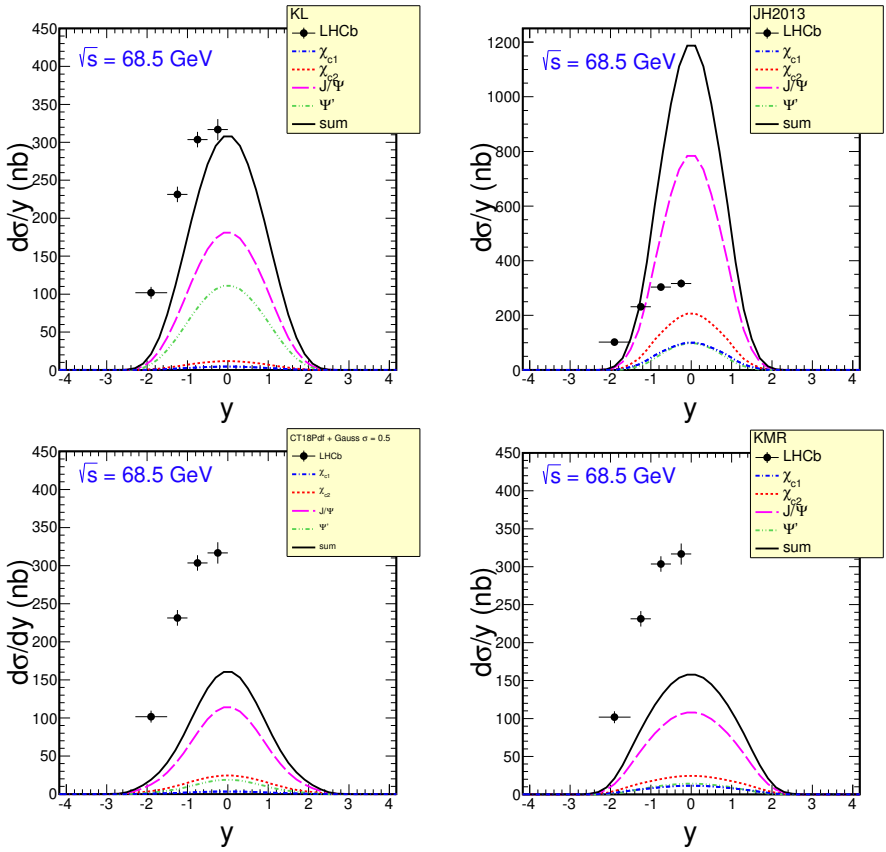

Fig. 9. Rapidity distribution of the J/ψ mesons for all considered mechanisms for different unintegrated gluon distribution functions.

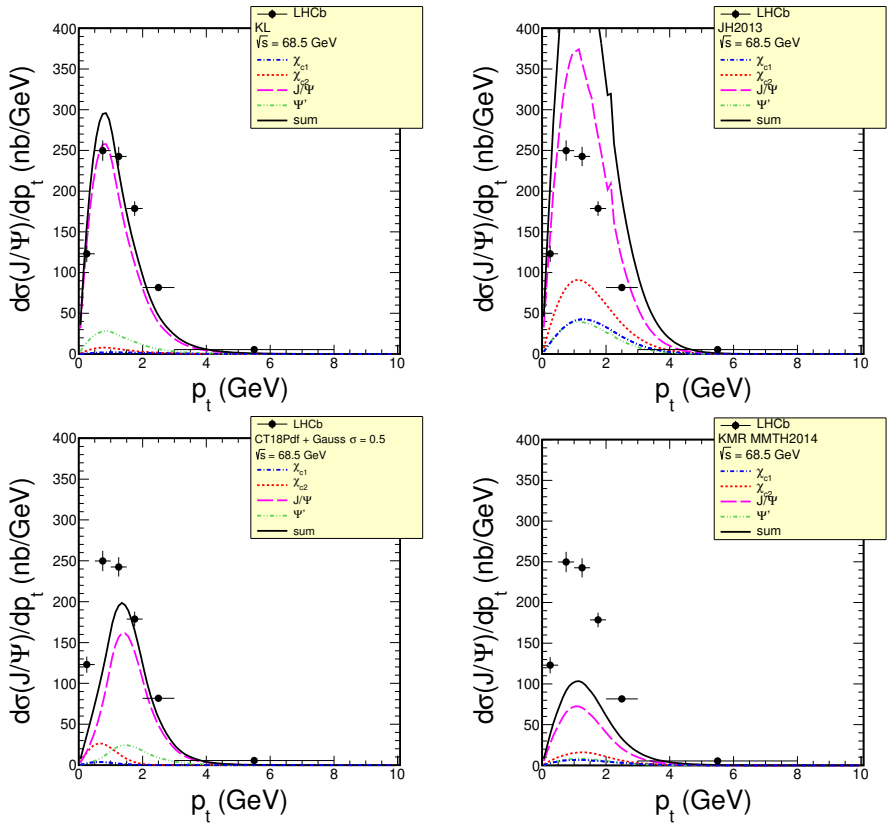

Fig. 10. Transverse momentum distribution of J/ψ mesons for all considered mechanisms for different unintegrated gluon distribution functions.

5. Conclusions

We have shown that the intrinsic charm and the recombination mechanisms are extremely important for forward charm production at energies much lower than the nominal LHC energies. A scenario proposed with the intrinsic-charm contribution is needed to describe the data points in the backward direction and at larger p_{t}s. We have found an upper limit for the intrinsic-charm probability P_{IC} ($\approx 0.5\%$) with the CT18FC. The recombination probability from the $D/\bar{D}$-production asymmetry ($\rho \approx 10\%$) has been found, consistent with earlier findings in the literature. The $D/\bar{D}$-production asymmetry in the backward region and at small transverse momenta has been explained by the recombination mechanism. The asymmetry at larger transverse momenta can be described neither by the recombination mechanism nor by the asymmetric intrinsic charm.

We have also analyzed prompt production of the J/ψ quarkonia for energies corresponding to fixed-target LHCb $p + A$ data at $\sqrt{s} = 68.5$ GeV. In this exploratory study, we have performed calculations within the k_t-factorization approach as we did previously in high-energy collisions. At high energies, one is sensitive to the region of very small x of the order of 10^{-4}, while here one is sensitive to much larger values of x_1 or x_2, typically larger than 10^{-2}. We have calculated distributions in rapidity and transverse momentum. The obtained results have been compared to the LHCb data. There is a relatively large spread of results for this intermediate-x region. The KMR and JH2013 UGDFs give a reasonable description of the data. Quite good result has been obtained with the KL UPDF used previously for light-charged particle production.

REFERENCES

[1] R. Maciuła, A. Szczurek, *Phys. Rev. D* **105**, 014001 (2022).
[2] S. Brodsky, P. Hoyer, C. Peterson, N. Sakai, *Phys. Lett. B* **93**, 451 (1980).
[3] R. Maciuła, A. Szczurek, *Phys. Rev. D* **107**, 034002 (2023).
[4] A. Cisek, A. Szczurek, *Phys. Rev. D* **97**, 034035 (2018).
[5] A. Cisek, A. Szczurek, a paper in preparation.
[6] E. Braaten, Y. Jia, T. Mehen, *Phys. Rev. Lett.* **89**, 122002 (2002).
[7] R. Maciuła, A. Szczurek, *Phys. Lett. B* **835**, 137530 (2022).
[8] V. Goncalves, R. Maciuła, A. Szczurek, *Phys. Rev. D* **110**, 074032 (2024).
[9] V. Goncalves, R. Maciuła, A. Szczurek, *Eur. Phys. J. C* **82**, 236 (2022).